Contemporary Mathematics
http://ojs.wiserpub.com/index.php/CM/

Research Article

Adopted Chebyshev Collocation Algorithm for Modeling Human Corneal Shape via the Caputo Fractional Derivative

Y. H. Youssri[1*], A. G. Atta[2]

[1] Department of Mathematics, Faculty of Science, Cairo University, Giza, 12613, Egypt
[2] Department of Mathematics, Faculty of Education, Ain Shams University, Roxy, Cairo, 11341, Egypt
E-mail: youssri@cu.edu.eg

Received: 10 January 2025; **Revised:** 31 January 2025; **Accepted:** 13 February 2025

Abstract: To solve a fractional boundary value problem that simulates the dynamics of the human corneal shape, we offer a semi-analytic spectral collocation procedure. The boundary conditions are exactly satisfied by expanding the proposed approximation solution as a finite sum of certain basis functions, namely a combination of the first kind Chebyshev polynomials. Next, using the typical Chebyshev nodes, we use the spectral collocation method and find explicit forms of the first- and second-order derivatives in both integer and fractional cases. At various values for orders of the fractional derivative and model parameter values, we display a number of graphical outcomes. We study the convergence and truncation error analysis of the proposed expansion. This paper presents a semi-analytic spectral technique to solve a fractional boundary value problem modeling human corneal dynamics. Using the Caputo fractional derivative and Chebyshev nodes, the solution is expanded as a finite sum of compact basis functions, with spectral collocation employed to derive explicit first- and second-order derivatives. Numerical simulations and convergence and error analyses are provided at various fractional orders and model parameters.

Keywords: fractional boundary value problem, Caputo fractional derivative, human corneal shape modeling, shifted Chebyshev polynomials, spectral collocation method

MSC: 65L10, 65M70, 33C45, 92C10, 26A33

1. Introduction

The intricate and subtle behavior of biological systems is difficult for classical calculus to capture since it takes integer-order derivatives into account. A more dynamic tool that enables the description of memory-effect events is fractional calculus [1–5]. Fractional derivatives are the most effective way to depict the cornea's slow shape changes over time [6]. The transparent dome covers the front of the human eye; the cornea; is responsible for focusing light and maintaining good vision. Sustaining its correct shape is vital for the best possible visual experience. Nonetheless, several variables may influence the cornea's form, potentially resulting in visual issues [7, 8].

Recently, many researchers offered a framework for modeling the human corneal shape using fractional calculus, for instance [9–13], this motivates us to develop a spectral semi-analytic approach to handle this model. This paves the way for further exploration of biological phenomena using the powerful tools of fractional calculus. Significant progress has

DOI: https://doi.org/10.37256/cm.6120256387

been made in this field by recent works like [14], which introduced a highly accurate matrix method for solving strongly nonlinear boundary value problems in corneal modeling, and [12], which introduced an integrated neuro-evolution-based solver for the dynamics of nonlinear corneal shape models. The properties and uses of Riemann-Liouville and Caputo derivatives [15], fractional integrability and differentiability [16], and the behavior of fractional derivatives in complex planes have all been extensively studied in the literature on fractional calculus [17], and various remarks on fractional derivative definitions and interpretations [18, 19]. To justify the transition from a nonlinear integer differential model to a fractional differential model, it is essential to recognize the capability of fractional derivatives to capture memory and hereditary effects, which are inherent in biological systems. The work by Okrasiński and Plociniczak [20] on nonlinear modeling of the corneal shape highlights the need for accurate and flexible mathematical frameworks. To better describe the intricate dynamics of the cornea, we build on their work by using fractional calculus, which offers a more robust and generalized modeling method.

Due to their special characteristics, Chebyshev polynomials are now a useful tool for solving a variety of differential equations. The optimality attribute of these polynomials is that they reduce error within a given interval. Because of this, they are very helpful in describing solutions to differential equations, particularly for those defined on a closed interval $[-1,\ 1]$. Moreover, a finite series of Chebyshev polynomials can be used to approximate solutions because of the simplicity of computing their explicit formulas of derivatives and their completeness inside the interval. The spectral method is a technique that greatly streamlines the solution procedure for a variety of scientific and engineering problems by converting complex differential equations into an algebraic equation system [21–25].

This study looks at new spectral procedures to study how the cornea changes shape. We use fractional calculus, which deals with non-whole numbers when we do differentiation and integration. We suggest a new way to model cornea shape changes using a kind of fractional calculus called the Caputo fractional derivative. This type of modeling includes a special part that's good for starting conditions. To solve the differential problem we get from this, for recent studies on numerical methods for differential problems, see [26, 27]. We use the shifted Chebyshev polynomials (SCPs) to help us construct the solution. These polynomials have traits that help them fit into the problem's rules easily. Also, we work out formulas for the first and second derivatives of these polynomials, both in the integer and the fractional case. This helps us use spectral collocation to find the desired spectral solution that's very close to what happens in real life. We depict graphs of the solution in different situations, with different numbers plugged in and different kinds of fractional derivatives. Finally, we look at how well our solutions are and check how much our approximate solutions are far from the unknown exact solution by controlling the residual error. For recent work on spectral methods for different mathematical models, please see [28–32].

We think that the novelty of our contribution of this paper can be summarized in the following items:

The employment of the introduced modified sets of SCPs of the first type in numerical analysis is new.

Derivations of some new theoretical results, such as the integer and fractional derivatives of the modified sets of SCPs of the first type.

A new study for the convergence analysis of the proposed expansion.

The remainder of the paper is structured as follows: The relevant features of first-kind Chebyshev polynomials are briefly described in Section 2, and the collocation spectral algorithm for numerically handling the suggested biological model is constructed in Section 3. We provide a thorough examination of the method's convergence and error analyses in Section 4. The results and debate are covered in Section 5, and Section 6 includes some closing thoughts.

2. An overview of the SCPs of the first type

The following three-term recurrence formula can be employed to construct the polynomials $T_{\ell}^{*}(z)$:

$$T_{\ell+1}^{*}(z) = 2\ (2z-1)\, T_{\ell}^{*}(z) - T_{\ell-1}^{*}(z),$$

where $T_0^*(z) = 1,\ T_1^*(z) = 2z - 1$.

The orthogonality property of $T_\ell^*(z)$ with the weight function $\hat{w}(z) = \dfrac{1}{\sqrt{z(1-z)}}$ is illustrated below [33, 34]:

$$\int_0^1 T_\ell^*(z) T_n^*(z) \hat{w}(z) dz = h_\ell \delta_{\ell,\, n},$$

where

$$h_\ell = \begin{cases} \pi, & \text{if } \ell = 0, \\ \dfrac{\pi}{2}, & \text{if } \ell > 0, \end{cases}$$

and

$$\delta_{\ell,\, n} = \begin{cases} 1, & \text{if } \ell = n, \\ 0, & \text{if } \ell \neq n. \end{cases}$$

Additionally, the power series representation of $T_\ell^*(z)$ and its inversion formula are [33, 34]:

$$T_\ell^*(z) = \ell \sum_{k=0}^{\ell} \frac{(-1)^{\ell-k} 2^{2k} (\ell + k - 1)!}{(\ell - k)!(2k)!} z^k,\ \ell > 0. \tag{1}$$

$$z^\ell = 2^{1-2\ell} (2\ell)! \sum_{p=0}^{\ell} \frac{\varepsilon_p}{(\ell - p)!(\ell + p)!}\, T_p^*(z),\ \ \ell \geq 0, \tag{2}$$

where

$$\varepsilon_\ell = \begin{cases} \dfrac{1}{2}, & \text{if } \ell = 0, \\ 1, & \text{if } \ell > 0. \end{cases} \tag{3}$$

The following linearization identity and connection relation [35] are vital in simplifying the derivatives of SCPs:

$$T_\ell^* T_n^* = \frac{1}{2} \left(T_{\ell+n}^* + T_{|\ell-n|}^* \right),\ \forall \ell,\ n \in \mathbb{N}. \tag{4}$$

$$DT_{\ell+1}^* = 2(\ell + 1) U_\ell^*,\ \forall \ell \in \mathbb{N}. \tag{5}$$

Corollary 1 [36] For any integer $q > 0$, the qth derivative of $T_\ell^*(z)$ can be rewritten in terms of their original polynomials as:

$$D^q T_\ell^*(z) = \sum_{\substack{p=0 \\ (\ell+p+q)\ even}}^{\ell-q} \varsigma_{\ell,\,p,\,q} T_p^*(z),$$

where

$$\varsigma_{\ell,\,p,\,q} = \frac{\ell 2^{2q} \varepsilon_p(q)_{\frac{1}{2}(\ell-p-q)}}{\left(\frac{1}{2}(\ell-p-q)\right)! \left(\frac{1}{2}(\ell+p+q)\right)_{1-q}},$$

and ε_p defined in (3).

3. A matrix collocation technique for the nonlinear fractional corneal shape equation

Herein, we analyze the following nonlinear fractional corneal shape model (NFCSM) [10]:

$$D^\beta u(\tau) - Au(\tau) + \frac{B}{\sqrt{1+D^\alpha u(\tau)^2}} = 0,\ \alpha \in]0,\ 1],\ \beta \in]1,\ 2],\ \tau \in [0,\ 1], \tag{6}$$

subject to the Dirichlet boundary constraints:

$$u'(0) = 0,\ u(1) = 0.$$

Here, $u(\tau)$ is a meridian of a surface of revolution demonstrating corneal geometry, and the coefficients $A,\ B$ are positive real integers that depend intimately on a variety of physical and biological parameters, including the corneal radius.

Remark 1 Equation (6) is solved under two specific scenarios corresponding to $\beta = 2,\ \alpha = 1,$ and $1 < \beta < 2, 0 < \alpha < 1$.

3.1 *Basis functions*

Let $\eta_i = \dfrac{4}{2i^2+1}$, and consider the basis functions defined as:

$$\lambda_i(\tau) = (1-\tau)\left(\frac{\eta_i}{4} + \tau\right) T_i^*(\tau). \tag{7}$$

Theorem 1 The following expressions hold:

$$\lambda_i(\tau) = \frac{1}{16}\left[T^*_{i-2}(\tau) - \eta_i T^*_{i-1}(\tau) + 2(1+\eta_i)T^*_i(\tau) - \eta_i T^*_{i+1}(\tau) + T^*_{i+2}(\tau)\right],$$

$$D\lambda_i(\tau) = \frac{1}{8}\left[2(1+\eta_i)iU_{i-1}(\tau) - \eta_i\left((i+1)U_i(\tau) + (i-1)U_{i-2}(\tau)\right) - \left((i+2)U_{i+1}(\tau) + (i-2)U_{i-3}(\tau)\right)\right],$$

$$D^2\lambda_i(\tau) = \frac{1}{32\tau(1-\tau)}[2(1+\eta_i)(\xi_{i+1}U_{i-2}(\tau) - \xi_i U_i(\tau)) - \eta_i(6iU_{i-1}(\tau) - \xi_{i+1}U_{i+1}(\tau)$$

$$+ \xi_i U_{i-3}(\tau)) - \xi_{i+3}U_i(\tau) + \xi_{i+2}U_{i+2}(\tau) - \xi_{i-1}U_{i-4}(\tau) + \xi_{i-2}U_{i-2}(\tau)],$$

where $\xi_i = i(i-1)$.

Proof. Starting from the inversion formula (2), we have

$$1 = \frac{1}{2}T^*_0,$$

$$\tau = \frac{1}{2}T^*_0 + \frac{1}{2}T^*_1,$$

$$\tau^2 = \frac{3}{8}T^*_0 + \frac{1}{2}T^*_1 + \frac{1}{8}T^*_2.$$

Now, $\lambda_i(\tau)$ can be written in terms of T^*_k as

$$\lambda_i = \left[\frac{\eta_i}{4}T^*_0 - \left(\frac{1}{2} + \frac{\eta_i}{8}\right)(T^*_0 + T^*_1) + \frac{3}{8}T^*_0 + \frac{1}{2}T^*_1 + \frac{1}{8}T^*_2\right]T^*_i.$$

Based on the linearization formula (see Eq. (4)), accordingly, we can represent $\lambda_i(\tau)$ in terms of T^*_k for $i-2 \le k \le i+2$ as

$$\lambda_i = \frac{1}{16}\left[T^*_{i-2} - \eta_i T^*_{i-1} + 2(1+\eta_i)T^*_i - \eta_i T^*_{i+1} + T^*_{i+2}\right].$$

Differentiating both sides w.r.t. τ, we get

$$D\lambda_i = \frac{1}{16}\left[DT^*_{i-2} - \eta_i DT^*_{i-1} + 2(1+\eta_i)DT^*_i - \eta_i DT^*_{i+1} + DT^*_{i+2}\right].$$

Now, applying Eq. (5), the desired derivatives are directly obtained. □

3.2 *Derivation of the collocation algorithm-classical integer derivatives*

Now, we consider the following function space

$$\Delta_N = \text{span}\{\lambda_\ell(\tau) : \ \ell = 0,\ 1,\ \ldots,\ N\}.$$

Then, any function $u_N(\tau) \in \Delta_N$ can be approximated as

$$u_N(\tau) \approx \sum_{\ell=0}^{N} \hat{u}_\ell \lambda_\ell(\tau). \tag{8}$$

Using (8), the residual $\mathbf{R}(\tau)$ of Eq. (6) can be written as

$$\mathbf{R}(\tau) = \sqrt{1+u_N'(\tau)^2}u_N''(\tau) - Au_N(\tau)\sqrt{1+u_N'(\tau)^2} + B$$

$$= \sqrt{1+\left(\sum_{\ell=0}^{N}\hat{u}_\ell\lambda_\ell'(\tau)\right)^2}\sum_{\ell=0}^{N}\hat{u}_\ell\lambda_\ell''(\tau) - A\sum_{\ell=0}^{N}\hat{u}_\ell\lambda_\ell(\tau)\sqrt{1+\left(\sum_{\ell=0}^{N}\hat{u}_\ell\lambda_\ell'(\tau)\right)^2} + B.$$

Using Theorem 1, one has

$$\mathbf{R}(\tau) = \sqrt{1+\left(\frac{1}{8}\sum_{\ell=0}^{N}\hat{u}_\ell\left[\begin{array}{l}2(1+\eta_\ell)\ell U_{\ell-1}(\tau) - \eta_\ell((\ell+1)U_\ell(\tau)+(\ell-1)U_{\ell-2}(\tau)) \\ -((\ell+2)U_{\ell+1}(\tau)+(\ell-2)U_{\ell-3}(\tau))\end{array}\right]\right)^2}$$

$$\left(\frac{1}{32\,\tau(1-\tau)}\sum_{\ell=0}^{N}\hat{u}_\ell\,[2(1+\eta_\ell)(\xi_{\ell+1}U_{\ell-2}(\tau)-\xi_\ell U_\ell(\tau)) - \eta_\ell(6\ell U_{\ell-1}(\tau) - \xi_{\ell+1}U_{\ell+1}(\tau)\right.$$

$$+\xi_\ell U_{\ell-3}(\tau)) - \xi_{\ell+3}U_\ell(\tau) + \xi_{\ell+2}U_{\ell+2}(\tau) - \xi_{\ell-1}U_{\ell-4}(\tau) + \xi_{\ell-2}U_{\ell-2}(\tau)]$$

$$\left.-\frac{A}{16}\sum_{\ell=0}^{N}\hat{u}_\ell\,\left[T_{\ell-2}^*(\tau) - \eta_\ell T_{\ell-1}^*(\tau) + 2(1+\eta_\ell)\,T_\ell^*(\tau) - \eta_\ell T_{\ell+1}^*(\tau) + T_{\ell+2}^*(\tau)\right]\right) + B.$$

The application of the collocation method yields $(N+1)$ algebraic equations system in the unknown expansion coefficients $\hat{u}_\ell$

$$\mathbf{R}(\tau_i) = 0,\ i = 1,\ 2,\ \ldots,\ N+1, \tag{9}$$

where the first roots of $T_i^*(\tau)$ are τ_i. Thus, the well-known Newton's iterative method can be employed to solve the system in (9) to find $\hat{u}_\ell$.

3.3 The derivation of the collocation algorithm when $1 < \beta < 2$ and $0 < \alpha < 1$

In this section, we introduce a numerical scheme for solving the NFCSM when $1 < \beta < 2$ and $0 < \alpha < 1$. First, we review some fundamental properties related to fractional calculus.

Definition 1 [37] The fractional derivative in the Caputo sense of order μ is defined as:

$$D^{\mu}h(\tau) = \frac{1}{\Gamma(m-\mu)}\int_0^{\tau}(\tau-\xi)^{m-\mu-1}h^{(m)}(\xi)d\xi,\ \mu > 0,\ \tau > 0,$$

where $m-1 < \mu \leq m,\ m \in \mathbb{N}$.

The following properties hold for the operator D^{μ} when $m-1 < \mu \leq m,\ m \in \mathbb{N}$:

$$D^{\mu}b = 0,\ b \text{ is a constant},$$

$$D^{\mu}z^m = \begin{cases} 0, & \text{if } m \in \mathbb{N}_0 \text{ and } m < \lceil \mu \rceil, \\ \dfrac{\Gamma(m+1)}{\Gamma(m-\mu+1)}z^{m-\mu}, & \text{if } m \in \mathbb{N}_0 \text{ and } m \geq \lceil \mu \rceil, \end{cases}$$

where $\mathbb{N} = \{1,\ 2,\ 3,\ ...\}$, $\mathbb{N}_0 = \{0\} \cup \mathbb{N}$ and $\lceil \mu \rceil$ represents the ceiling function.

Theorem 2 The following formula holds for all $\alpha \in (0,\ 1)$:

$$D^{\alpha}\lambda_j(\tau) = \tau^{-\alpha}\left(\sum_{k=1}^{j}\sum_{i=0}^{k}\mathscr{F}^1_{i,\,k,\,j}T^*_i(\tau) + \sum_{k=0}^{j}\sum_{i=0}^{k+1}\mathscr{F}^2_{i,\,k,\,j}T^*_i(\tau) + \sum_{k=0}^{j}\sum_{i=0}^{k+2}\mathscr{F}^3_{i,\,k,\,j}T^*_i(\tau)\right), \tag{10}$$

where

$$\mathscr{F}^1_{i,\,k,\,j} = \frac{2j\varepsilon_i(-1)^{j-k}\Gamma(k+1)\Gamma(j+k)}{(2j^2+1)\Gamma(-i+k+1)\Gamma(i+k+1)\Gamma(j-k+1)\Gamma(k-\alpha+1)},$$

$$\mathscr{F}^2_{i,\,k,\,j} = \frac{2j^3(k+1)(2k+1)\varepsilon_i(-1)^{j-k}\Gamma(k+2)\Gamma(j+k)}{(2j^2+1)\Gamma(-i+k+2)\Gamma(i+k+2)\Gamma(j-k+1)\Gamma(k-\alpha+2)},$$

$$\mathscr{F}^3_{i,\,k,\,j} = \frac{j\varepsilon_i(-1)^{j-k}\Gamma(k+3)\Gamma(2k+5)\Gamma(j+k)}{8(2k)!(j-k)!\Gamma(-i+k+3)\Gamma(i+k+3)\Gamma(k-\alpha+3)}.$$

Proof. The power form representation of $\lambda_j(\tau)$ can be written, after using relation (1), as

$$D_\tau^\alpha \lambda_j(\tau) = \frac{1}{2j^2+1}\sum_{k=1}^{j}\frac{j2^{2k}k!(-1)^{j-k}(j+k-1)!}{(2k)!(j-k)!(k-\alpha)!}\tau^{k-\alpha}$$

$$+\frac{2j^2}{2j^2+1}\sum_{k=0}^{j}\frac{j2^{2k}(k+1)!(-1)^{j-k}(j+k-1)!}{(2k)!(j-k)!(-\alpha+k+1)!}\tau^{-\alpha+k+1}$$

$$-\sum_{k=0}^{j}\frac{j2^{2k}(k+2)!(-1)^{j-k}(j+k-1)!}{(2k)!(j-k)!(-\alpha+k+2)!}\tau^{-\alpha+k+2}.$$

By applying the inversion formula (2) and simplifying the result, we obtain the desired expression in (10). □

Theorem 3 The following formula holds for all $\beta \in (1,\ 2)$:

$$D^\beta \lambda_j(\tau) = \tau^{-\beta}\left(\sum_{k=2}^{j}\sum_{i=0}^{k}\mathscr{G}^1_{i,\,k,\,j}T_i^*(\tau)+\sum_{k=1}^{j}\sum_{i=0}^{k+1}\mathscr{G}^2_{i,\,k,\,j}T_i^*(\tau)+\sum_{k=0}^{j}\sum_{i=0}^{k+2}\mathscr{G}^3_{i,\,k,\,j}T_i^*(\tau)\right),$$

where

$$\mathscr{G}^1_{i,\,k,\,j} = \frac{2j\varepsilon_i(-1)^{j-k}\Gamma(k+1)\Gamma(j+k)}{(2j^2+1)\Gamma(-i+k+1)\Gamma(i+k+1)\Gamma(j-k+1)\Gamma(k-\beta+1)},$$

$$\mathscr{G}^2_{i,\,k,\,j} = \frac{2j^3(k+1)(2k+1)\varepsilon_i(-1)^{j-k}\Gamma(k+2)\Gamma(j+k)}{(2j^2+1)\Gamma(-i+k+2)\Gamma(i+k+2)\Gamma(j-k+1)\Gamma(k-\beta+2)},$$

$$\mathscr{G}^3_{i,\,k,\,j} = \frac{j\varepsilon_i(-1)^{j-k}\Gamma(k+3)\Gamma(2k+5)\Gamma(j+k)}{8(2k)!(j-k)!\Gamma(-i+k+3)\Gamma(i+k+3)\Gamma(k-\beta+3)}.$$

Proof. The proof of this theorem follows the same steps as in Theorem 2, but adapted for the case where $\beta \in (1,\ 2)$.□
By virtue of (8) along with Theorems 2 and 3, the residual $\mathbf{R}(\tau)$ of Eq. (6) is given by

$$\mathbf{R}(\tau) = \sqrt{1+D^\alpha u_N(\tau)^2}D^\beta u_N(\tau) - Au_N(\tau)\sqrt{1+D^\alpha u_N(\tau)^2}+B$$

$$= \sqrt{1+\left(\sum_{\ell=0}^{N}\hat{u}_\ell D^\alpha \lambda_\ell(\tau)\right)^2}\sum_{\ell=0}^{N}\hat{u}_\ell D^\beta\lambda_\ell(\tau) - A\sum_{\ell=0}^{N}\hat{u}_\ell\lambda_\ell(\tau)\sqrt{1+\left(\sum_{\ell=0}^{N}\hat{u}_\ell D^\alpha\lambda_\ell(\tau)\right)^2}+B$$

$$= \sqrt{1+\left(\sum_{\ell=0}^{N}\hat{u}_\ell\tau^{-\alpha}\left(\sum_{k=1}^{\ell}\sum_{i=0}^{k}\mathscr{F}^1_{i,\,k,\,\ell}T_i^*(\tau)+\sum_{k=0}^{\ell}\sum_{i=0}^{k+1}\mathscr{F}^2_{i,\,k,\,\ell}T_i^*(\tau)+\sum_{k=0}^{\ell}\sum_{i=0}^{k+2}\mathscr{F}^3_{i,\,k,\,\ell}T_i^*(\tau)\right)\right)^2}$$

$$\times \sum_{\ell=0}^{N} \hat{u}_\ell \tau^{-\beta} \left(\sum_{k=2}^{\ell} \sum_{i=0}^{k} \mathscr{G}^1_{i,\,k,\,\ell} T_i^*(\tau) + \sum_{k=1}^{\ell} \sum_{i=0}^{k+1} \mathscr{G}^2_{i,\,k,\,\ell} T_i^*(\tau) + \sum_{k=0}^{\ell} \sum_{i=0}^{k+2} \mathscr{G}^3_{i,\,k,\,\ell} T_i^*(\tau) \right)$$

$$- \frac{A}{16} \sum_{\ell=0}^{N} \hat{u}_\ell \left(T^*_{\ell-2}(\tau) - \eta_\ell T^*_{\ell-1}(\tau) + 2(1+\eta_\ell) T^*_\ell(\tau) - \eta_\ell T^*_{\ell+1}(\tau) + T^*_{\ell+2}(\tau) \right)$$

$$\times \sqrt{1 + \left(\sum_{\ell=0}^{N} \hat{u}_\ell \tau^{-\alpha} \left(\sum_{k=1}^{\ell} \sum_{i=0}^{k} \mathscr{F}^1_{i,\,k,\,\ell} T_i^*(\tau) + \sum_{k=0}^{\ell} \sum_{i=0}^{k+1} \mathscr{F}^2_{i,\,k,\,\ell} T_i^*(\tau) + \sum_{k=0}^{\ell} \sum_{i=0}^{k+2} \mathscr{F}^3_{i,\,k,\,\ell} T_i^*(\tau) \right) \right)^2} + B.$$

Applying the collocation method at the first roots of $T_i^*(\tau)$ $\{\tau_i : i = 1,\ 2,\ ...,\ N+1\}$, we get

$$\mathbf{R}(\tau_i) = 0,\ i = 1,\ 2,\ ...,\ N+1.$$

Newton's iterative method can be employed to solve a system of $(N+1)$ nonlinear algebraic equations to obtain the unknown expansion coefficients $\hat{u}_\ell$.

4. Error estimate

Lemma 1 The following inequality holds for $\lambda_j(t)$

$$|\lambda_j(t)| < 2,\ \forall j \geq 0.$$

Proof. The definition of $\lambda_j(t)$ in (7) can be written as

$$\lambda_j(t) = \left(\frac{(2j^2)}{2j^2+1} + \frac{1}{2j^2+1} x - x^2 \right) T_j^*(t).$$

Now, taking the absolute value for each side and using the two identities $|T_j^*(t)| \leq 1$, and $|t| < 1$, we get the desired result. □

Theorem 4 [36] If $g(t) \in C^q(0,\ \tau),\ \tau > 0$, such that $g^{(q)}(t)$ is bounded for some $q > 3$ and $g(t)$ is approximated as

$$g(t) \approx g_N(t) = \sum_{i=0}^{N} a_i T_i^*(t),$$

then, the following bound on a_i holds

$$|a_i| = O(i^{-q}),\ \forall i > 1.$$

Corollary 2 The following bound on $\hat{u}_\ell$ holds if $u(t) = (1-t)\left(\frac{\eta_\ell}{4}+t\right) g(t) \in C^q(0,\ 1),\ \ell \geq 0$, such that $u^{(q)}(t)$ is bounded for some $q > 3$ and $u(t)$ is approximated as in (8).

$$|\hat{u}_\ell| = O(\ell^{-q}),\ \forall \ell > 1.$$

Proof. The assumption of this corollary along with Theorem 4 enables us to write

$$u(t) = (1-t)\left(\frac{\eta_\ell}{4}+t\right) g(t) = (1-t)\left(\frac{\eta_\ell}{4}+t\right) \sum_{\ell=0}^{\infty} a_\ell T_\ell^*(t) = \sum_{\ell=0}^{\infty} \hat{u}_\ell \lambda_\ell(t).$$

Now, the application of Theorem 4 leads to

$$|\hat{u}_\ell| = |a_\ell| = O(\ell^{-q}),\ \forall \ell > 1.$$

This completes the proof of this corollary. □

Theorem 5 The following error estimate is true

$$|u(t) - u_N(t)| = O(N^{1-q}).$$

Proof. Based on the definition of $u(t)$ and $u_N(t)$, one can write

$$u(t) - u_N(t) = \sum_{\ell=N+1}^{\infty} \hat{u}_\ell \lambda_\ell(t).$$

Now, using the following inequality $|\lambda_\ell(t)| < 2$, along with Corollary 2, one has

$$|u(t) - u_N(t)| = \left| \sum_{\ell=N+1}^{\infty} \hat{u}_\ell \lambda_\ell(t) \right|$$

$$< \sum_{\ell=N+1}^{\infty} \frac{2}{\ell^q} = 2\zeta(q,\ N+1) = O(N^{1-q}).$$

where $\zeta(q,\ N+1)$ is the Hurwitz zeta function [38]. This completes the proof of this theorem. □

5. Results and discussion

This section is devoted to check the applicability and accuracy of our proposed scheme.
Let's define the following absolute residual errors norm and the maximum absolute residual errors

$$RES = \left| \sqrt{1+D^{\alpha}u_N(t)^2}D^{\beta}u_N(t) - Au_N(t)\sqrt{1+D^{\alpha}u_N(t)^2} + B \right|,$$

$$MRES = \max_{t\in(0,\,1)} \left| \sqrt{1+D^{\alpha}u_N(t)^2}D^{\beta}u_N(t) - Au_N(t)\sqrt{1+D^{\alpha}u_N(t)^2} + B \right|.$$

Now, if we consider the successive errors E_N, and E_{N+1}, then the order of convergence for the given method can be calculated as

$$\text{Order} = \frac{\log \dfrac{E_{N+1}}{E_N}}{\log \dfrac{N+1}{N}}.$$

When $\beta = 2$ and $\alpha = 1$, the MREs at various values of $A,\ B$, and N are displayed in Tables 1 and 2. This shows how accurate our approach is. Also, they verifies that the suggested approach reduces errors consistently throughout the domain. Table 3, shows the MREs and order of convergence at $A = 1,\ B = 1$ and $\beta = 2,\ \alpha = 1$. A comparison of the REs at $\beta = 2$ and $\alpha = A = B = 1$, between current technique at $N = 19$ and the method in [10] at $N = 15$ is shown in Table 4. This comparison reveal the superior performance of our technique over method in [10]. The approximate solution (right) and REs (left) are shown in Figure 1 when $A = 0.5,\ B = 0.5,\ \alpha = 1$ and $\beta = 2$ at $N = 12$. This figure verifies that the suggested approach reduces errors consistently throughout the domain. Furthermore, when $N = 6$ at various values of A and B, Figures 2-5 demonstrate that approximate solutions have smaller variations of different values of α and β around the values $\alpha = 1,\ \beta = 2$. The results demonstrate the effect of the parameters A and B, which are related to the radius of the cornea, on the corneal geometry. The model's capability also provides deeper insights into corneal biomechanics, making it valuable for applications such as diagnosis and treatment of corneal disorders.

Table 1. The MREs at $\beta = 2,\ \alpha = 1$

N	$A = 1,\ B = 1$	$A = 1.3,\ B = 1.6$	$A = 0.8,\ B = 1.1$
3	2.4231×10^{-3}	1.13387×10^{-2}	1.01765×10^{-3}
6	1.38556×10^{-5}	4.47518×10^{-4}	8.74918×10^{-6}
9	1.77522×10^{-7}	8.60545×10^{-6}	8.73423×10^{-7}
12	1.17822×10^{-9}	1.44607×10^{-7}	1.87596×10^{-8}
15	4.96152×10^{-12}	2.08988×10^{-9}	2.87627×10^{-10}
18	8.43334×10^{-15}	2.43155×10^{-11}	3.70726×10^{-12}
21	1.33657×10^{-14}	6.55032×10^{-15}	6.6025×10^{-15}

Table 2. The MREs at $\beta = 2,\ \alpha = 1$

N	$A = 1.4,\ B = 1.8$	$A = 1.5,\ B = 1.9$	$A = 1.7,\ B = 1.2$
3	2.5606×10^{-2}	3.06831×10^{-2}	4.21816×10^{-2}
6	1.27271×10^{-3}	1.67124×10^{-3}	2.21062×10^{-3}
9	3.85178×10^{-5}	5.51176×10^{-5}	8.17376×10^{-5}
12	1.06888×10^{-6}	1.65986×10^{-6}	2.72582×10^{-6}
15	2.79866×10^{-8}	4.70011×10^{-8}	8.47925×10^{-8}
18	7.17118×10^{-10}	1.29848×10^{-9}	2.55483×10^{-9}
21	7.96502×10^{-12}	1.53422×10^{-11}	3.24917×10^{-11}
24	2.02013×10^{-13}	8.97893×10^{-14}	6.21005×10^{-13}

Table 3. The MREs and order of convergence at $A = 1,\ B = 1$ and $\beta = 2,\ \alpha = 1$

N	Error	Order	N	Error	Order
3	2.4231×10^{-3}	-	11	3.6368×10^{-9}	1.05694
4	4.17743×10^{-4}	1.02379	12	1.17822×10^{-9}	1.02095
5	8.30212×10^{-5}	1.04023	13	1.63196×10^{-11}	1.17045
6	1.38556×10^{-5}	1.04696	14	3.76343×10^{-11}	0.93922
7	4.84252×10^{-6}	1.00731	15	4.96148×10^{-12}	1.05679
8	1.75522×10^{-7}	1.37985	16	6.51368×10^{-13}	1.05291
9	1.47522×10^{-7}	1.07287	17	2.40474×10^{-13}	1.01335
10	2.1515×10^{-8}	1.07104	18	8.54872×10^{-15}	1.01512

Table 4. Comparison of the REs at $\beta = 2,\ \alpha = A = B = 1$

t	Method in [10] at $N = 15$	Present method at $N = 19$
0	0.000002052	2.22045×10^{-16}
0.1	0.000001962	2.22045×10^{-16}
0.2	0.000002037	2.22045×10^{-16}
0.3	0.000002102	1.11022×10^{-16}
0.4	0.000002127	4.44089×10^{-16}
0.58	0.000002184	3.33067×10^{-16}
0.6	0.000002265	3.33067×10^{-16}
0.7	0.000002325	1.11022×10^{-16}
0.88	0.000002388	1.11022×10^{-16}
0.9	0.000002117	1.11022×10^{-16}
1	0	1.68754×10^{-14}

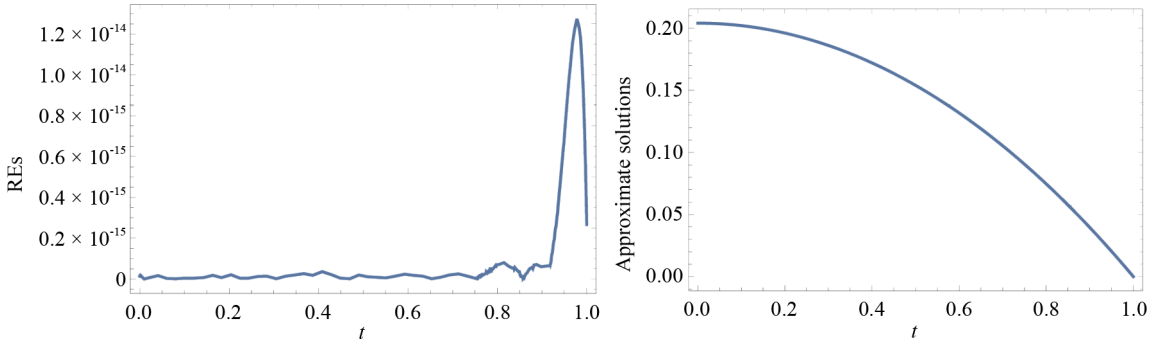

Figure 1. The REs (left) and approximate solution (right) when $A = 0.5,\ B = 0.5$ at $N = 12$

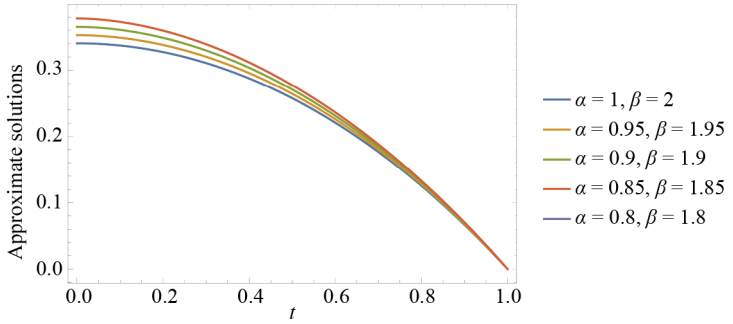

Figure 2. The approximate solutions when $A = 1,\ B = 1$ at $N = 6$

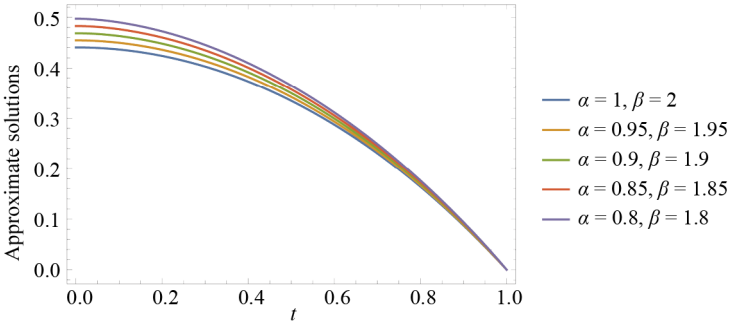

Figure 3. The approximate solutions when $A = 1.72,\ B = 1.6$ at $N = 6$

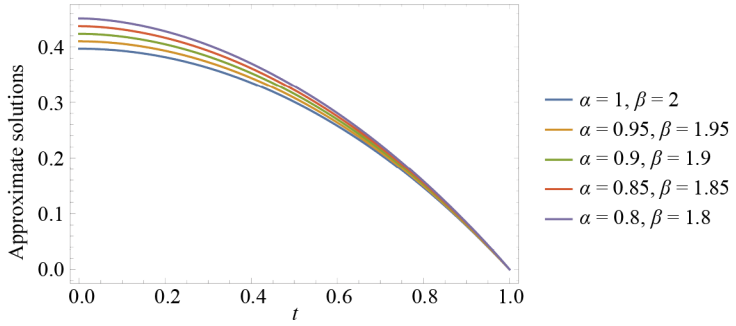

Figure 4. The approximate solutions when $A = 1.38,\ B = 1.31$ at $N = 6$

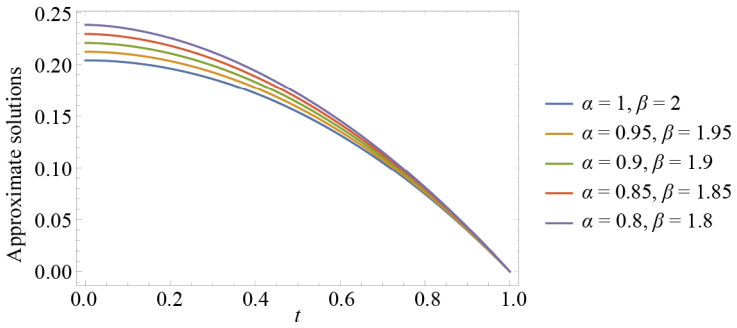

Figure 5. The approximate solutions when $A = B = 0.5$ at $N = 6$

6. Concluding remarks

We have constructed a spectral semi-analytic procedures in this work to spectrally solve the nonlinear fractional model of the human corneal shape. Convergence and truncation error analysies were used to show the method's accuracy. This work demonstrates how spectral approaches may be applied to intricate biological systems and increases our understanding of corneal dynamics through the use of fractional calculus. To stress on the importance of our suggested methodology, future research could investigate adapting the concept to other biological systems with fractional dynamics, incorporate more intricate models, and create more effective computational numerical spectral methods for large-scale differential models. Furthermore, real-time simulations can be made possible by combining the technique with optimization problems on the parameter of orthogonal polynomials, and applying it to 3D human eye models could improve predictions of changes in corneal shape. As an expected future work, we aim to employ the developed theoretical results in this paper along with suitable spectral methods to treat some other problems.

Conflict of interest

The authors declare that there is no conflict of interest.

References

[1] Hilfer R. *Applications of Fractional Calculus in Physics*. World scientific; 2000.

[2] Butzer PL, Westphal U. An introduction to fractional calculus. In: *Applications of Fractional Calculus in Physics*. World Scientific; 2000. p.1-85.

[3] Sabatier J, Agrawal OP, Machado JT. *Advances in Fractional Calculus*. Springer; 2007.
[4] Ross B. The development of fractional calculus 1695-1900. *Historia Mathematica*. 1977; 4(1): 75-89.
[5] Gorenflo R, Mainardi F. *Fractional Calculus: Integral and Differential Equations of Fractional Order*. Springer; 1997.
[6] Mandal D, Chattopadhyay H, Halder K. Constitutive modeling of human cornea through fractional calculus approach. *Physics of Fluids*. 2023; 35(3): 031907.
[7] Nishida T, Saika S. Cornea and sclera: anatomy and physiology. *Cornea*. 2010; 1: 3-24.
[8] Okrasiński W, Płociniczak Ł. A nonlinear mathematical model of the corneal shape. *Nonlinear Analysis: Real World Applications*. 2012; 13(3): 1498-1505.
[9] Erturk VS, Ahmadkhanlu A, Kumar P, Govindaraj V. Some novel mathematical analysis on a corneal shape model by using Caputo fractional derivative. *Optik*. 2022; 261: 169086.
[10] Abukhaled M, Abukhaled Y. Efficient semianalytical investigation of a fractional model describing human cornea shape. *Modeling and Artificial Intelligence in Ophthalmology*. 2024; 6(1): 1-15.
[11] Waseem W, Sulaiman M, Alhindi A, Alhakami H. A soft computing approach based on fractional order DPSO algorithm designed to solve the corneal model for eye surgery. *IEEE Access*. 2020; 8: 61576-61592.
[12] Ahmad I, Raja MAZ, Ramos H, Bilal M, Shoaib M. Integrated neuro-evolution-based computing solver for dynamics of nonlinear corneal shape model numerically. *Neural Computing and Applications*. 2021; 33(11): 5753-5769.
[13] Waseem W, Sulaiman M, Alhindi A, Alhakam H. A soft computing approach based on fractional order dpso algorithm designed to solve the corneal model for eye surgery. *IEEE Access*. 2020; 8: 61576-61592.
[14] Abbasi Z, Izadi M, Hosseini MM. A highly accurate matrix method for solving a class of strongly nonlinear BVP arising in modeling of human shape corneal. *Mathematical Methods in the Applied Sciences*. 2023; 46(2): 1511-1527.
[15] Li C, Qian D, Chen Y. On Riemann-Liouville and caputo derivatives. *Discrete Dynamics in Nature and Society*. 2011; 2011(1): 562494.
[16] Li C, Zhao Z. Introduction to fractional integrability and differentiability. *The European Physical Journal Special Topics*. 2011; 193(1): 5-26.
[17] Li C, Dao X, Guo P. Fractional derivatives in complex planes. *Nonlinear Analysis: Theory, Methods and Applications*. 2009; 71(5-6): 1857-1869.
[18] Li C, Deng W. Remarks on fractional derivatives. *Applied Mathematics and Computation*. 2007; 187(2): 777-784.
[19] Youssri YH. Orthonormal ultraspherical operational matrix algorithm for fractal-fractional Riccati equation with generalized Caputo derivative. *Fractal and Fractional*. 2021; 5(3): 100.
[20] Pociniczak L, Okrasinski W, Nieto JJ, Dominguez O. On a nonlinear boundary value problem modeling corneal shape. *Journal of Mathematical Analysis and Applications*. 2014; 414(1): 461-471.
[21] Youssri YH, Atta AG. Modal spectral Tchebyshev Petrov-Galerkin stratagem for the time-fractional nonlinear Burgers' equation. *Iranian Journal of Numerical Analysis and Optimization*. 2024; 14(1): 167-190.
[22] Youssri YH, Atta AG, Moustafa MO, Abu Waar ZY. *Explicit Collocation Algorithm for the Nonlinear Fractional Duffing Equation via Third-Kind Chebyshev Polynomials*. Ferdowsi University of Mashhad; 2025.
[23] Abdelhakem M, Abdelhamied D, El-kady M, Youssri YH. Enhanced shifted Tchebyshev operational matrix of derivatives: two spectral algorithms for solving even-order BVPs. *Journal of Applied Mathematics and Computing*. 2023; 69(5): 3893-3909.
[24] Youssri YH, Abd-Elhameed WM, Elmasry AA, Atta AG. An efficient petrov-galerkin scheme for the euler-bernoulli beam equation via second-kind chebyshev polynomials. *Fractal and Fractional*. 2025; 9(2): 78.
[25] Sayed SM, Mohamed AS, Abo-Eldahab EM, Youssri YH. Spectral framework using modified shifted Chebyshev polynomials of the third-kind for numerical solutions of one-and two-dimensional hyperbolic telegraph equations. *Boundary Value Problems*. 2025; 2025: 7.
[26] Waseem, Ullah A, Awwad FA, Ismail EA. Analysis of the corneal geometry of the human eye with an artificial neural network. *Fractal and Fractional*. 2023; 7(10): 764.
[27] Ilyas H, Ahmad I, Hussain SI, Shoaib M, Raja MAZ. Design of evolutionary computational intelligent solver for nonlinear corneal shape model by Mexican Hat and Gaussian wavelet neural networks. *Waves in Random and Complex Media*. 2024; 2024: 1-23.

[28] Izadi M, Ansari KJ, Srivastava HM. A highly accurate and efficient Genocchi-based spectral technique applied to singular fractional order boundary value problems. *Mathematical Methods in the Applied Sciences*. 2025; 48(1): 905-925.
[29] Zhu J, Ullah M, Ullah S, Riaz MB, Saqib AB, Alamri AM, et al. A novel numerical solution of nonlinear stochastic model for the propagation of malicious codes in Wireless Sensor Networks using a high order spectral collocation technique. *Scientific Reports*. 2025; 15(1): 228.
[30] Celik I. Gegenbauer wavelet collocation method for the fractional unsteady squeezing flow of casson fluid. *International Journal of Applied and Computational Mathematics*. 2025; 11(1): 15.
[31] Youssri YH, Atta AG. Chebyshev petrov-galerkin method for nonlinear time-fractional integro-differential equations with a mildly singular kernel. *Journal of Applied Mathematics and Computing*. 2025; 2025: 1-21.
[32] Yassin NM, Aly EH, Atta AG. Novel approach by shifted Schröder polynomials for solving the fractional Bagley-Torvik equation. *Physica Scripta*. 2024; 100(1): 015242.
[33] Moustafa M, Youssri YH, Atta AG. Explicit Chebyshev Galerkin scheme for the time-fractional diffusion equation. *International Journal of Modern Physics C*. 2024; 35(01): 1-15.
[34] Atta AG, Youssri YH. Advanced shifted first-kind Chebyshev collocation approach for solving the nonlinear time-fractional partial integro-differential equation with a weakly singular kernel. *Computational and Applied Mathematics*. 2022; 41(8): 381.
[35] Mason JC, Handscomb DC. *Chebyshev Polynomials*. Chapman and Hall/CRC; 2002.
[36] Abd-Elhameed WM, Machado JAT, Youssri YH. Hypergeometric fractional derivatives formula of shifted Chebyshev polynomials: tau algorithm for a type of fractional delay differential equations. *International Journal of Nonlinear Sciences and Numerical Simulation*. 2022; 23(7-8): 1253-1268.
[37] Podlubny I. *Fractional Differential Equations: An Introduction to Fractional Derivatives, Fractional Differential Equations, to Methods of Their Solution and Some of Their Applications*. Elsevier; 1998.
[38] Berndt BC. On the Hurwitz zeta-function. *The Rocky Mountain Journal of Mathematics*. 1972; 2(1): 151-157.